AFDEX Newsletter Q4 / 2018

MFRC
www.afdex.com, mfrc@afdex.com
Tel: +82-55-755-7529, Fax: +82-55-761-7529

1. Optimal process design

1.1 Grain flow line function, density, density gradient

Recently, with the development of metal forming CAE technology, the demand for process optimal design from AFDEX users is increasing. This is a natural trend. Optimal design of metal forming processes is very difficult and it is not easy to estimate the correlation between the design variables. Even if the metal forming CAE technology is used efficiently, if someone does not have a lot of experience, trial and error is required, which is still a burden on engineers. This is a challenging situation and solutions have to be developed in a gradual fashion. Currently optimization is partially possible, of course with some limitations.

The fundamental factor that has inhibited the optimal design of the metal forming process is the grain flow lines. Along with the forming load, the grain flow lines are a key factor in the metal forming process design. The calculation time and design parameterization of the die geometry is one of the many other problems, but it is not a fundamental problem.

Fig. 1.1 2D Grain flow lines

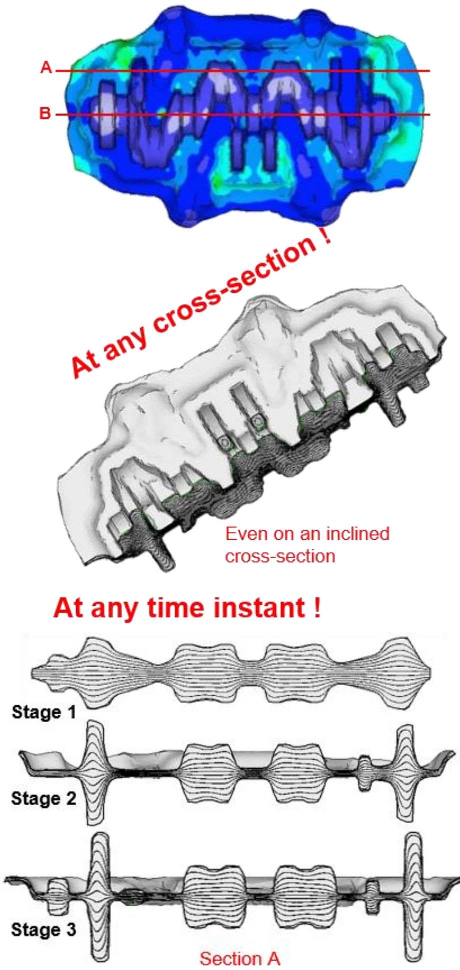

Fig. 1.2 3D Grain flow lines

Since five years, AFDEX has been providing a visualization technique for 3D grain flow lines (MS Joun, MC Lee, JG Eom, 2016, Simulation device for object to be plastically deformed, JP-Patent 5967493). Figure 1.1 and Figure 1.2 show typical applications.

Utilizing the visualization capabilities of the grain flow lines, engineers have facilitated the evaluation of process design. However, it does not solve the bottleneck problem of optimal design by itself. Recently, GNU and MFRC has developed a quantification method for metal flow lines. The line itself is defined as the contour line of the initial coordinates of the current node, the gradient of the initial coordinates is defined as the grain flow density vector, and the gradient of the grain flow density is defined as the overlapping index. Figure 1.3, Figure 1.4, and Figure 1.5 show the grain flow line function, its density, and its density gradient.

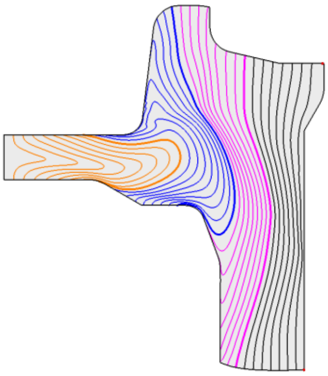

Fig. 1.3 Grain flow lines

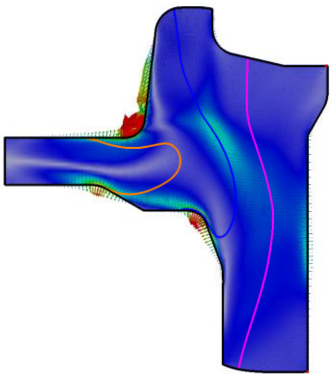

Fig. 1.4 Density of grain flow lines

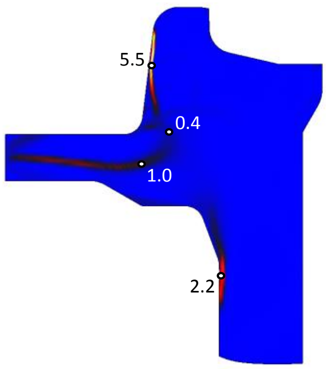

Fig. 1.5 Density gradient of grain flow lines

1.2 Application of optimal design considering grain flow lines

Figure 1.6 shows an example of optimal design of the forging process of the outer ring of a first-generation hub bearing. The objective function is the difference of grain flow line function values calculated at two symmetric points. Figure 1.6 compares the grain flow lines of the initial and optimal designs. As shown in this figure, the grain flow lines satisfying the up-down symmetry condition was obtained by performing optimal design without user intervention (KSTP Fall Conference, Jeju Island, 2018.10.11).

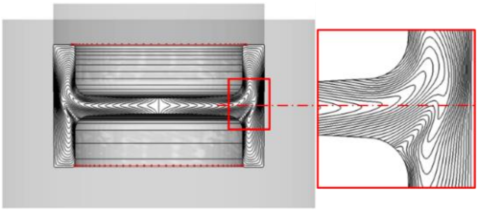

(a) Initial design

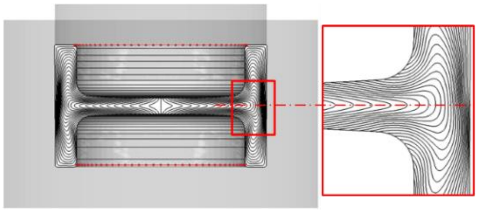

(b) Optimal design

Fig. 1.6 Optimal process design of the first-generation hub bearing outer ring

Figure 1.7 shows the outer ring of a tapered roller bearing with a flange. The grain flow lines of the inner inclined surface of the outer ring to which the taper roller contacts, should be parallel to the surface which would be formed by cutting. This can be done by taking the inner product of the grain flow density vector (the gradient of the grain flow function) and the unit normal vector on the surface as the objective function. Figure 1.7 compares the initial design with the optimal design (KSTP Fall Conference, Jeju Island, 2018.10.11).

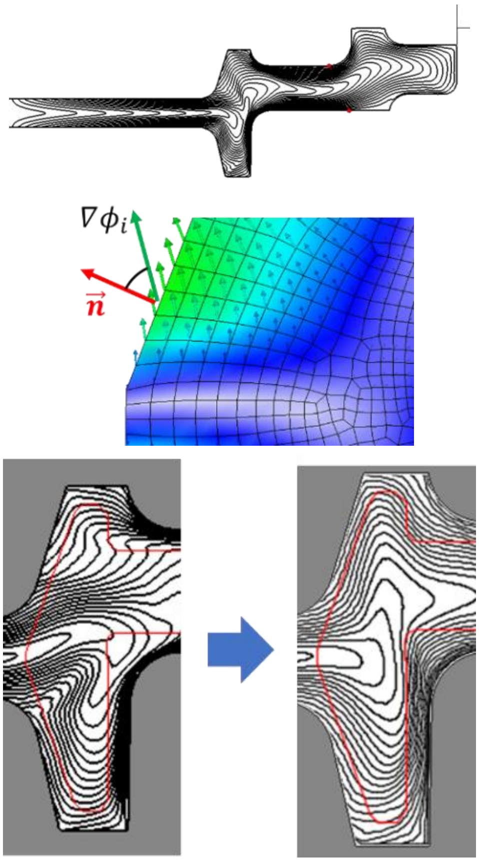

Fig. 1.7 Outer ring of a tapered roller bearing with flange

Figure 1.8. shows an example of optimal design to prevent the local sinking of grain flow lines. In consideration of the characteristics of local sinking of grain flow lines, the objective function is defined using the grain flow density and overlapping index, which are defined in two directions (Fig. 1.9-11). In the objective function, the effective strain and maximum forming load are also considered as a weight and constraint equation is used to maintain the gap of the flash unit constant.

As shown in Figure 1.9, local sinking defects tend to be locally reduced in two directions at the same time, and the overlapping index is also different from those shown in Figure 1.8. We have proposed and used an objective function considering these features.

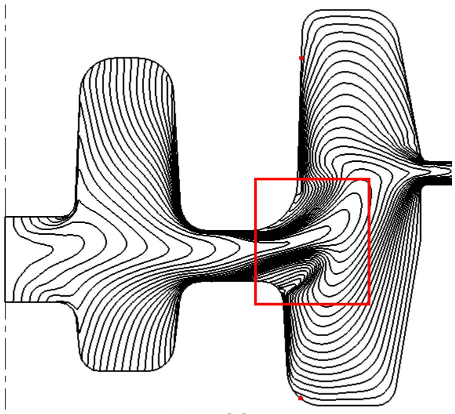

(a) Initial design

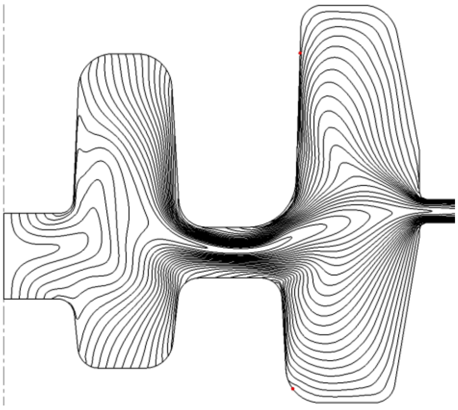

(b) Optimal design

Fig. 1.8 Optimal process design considering local sinking

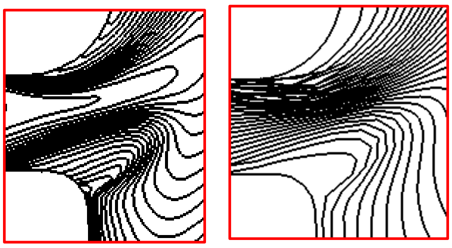

Fig. 1.9 Objective function

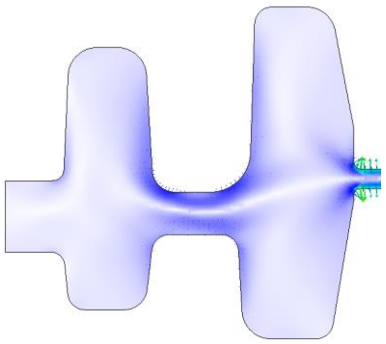

(a) Vertical direction

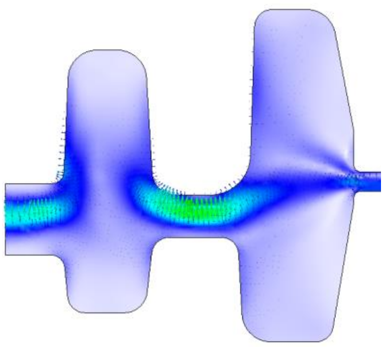

(b) Horizontal direction

Fig. 1.10 Grain flow density

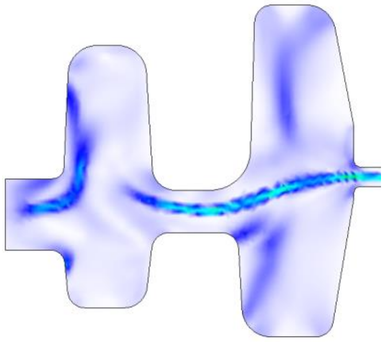

(a) Vertical direction

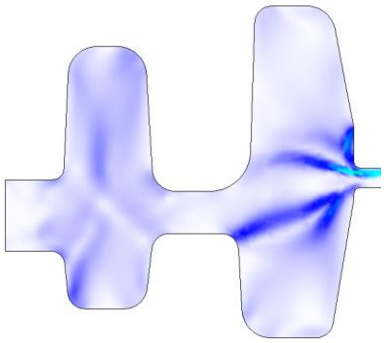

(b) Horizontal direction

Fig. 1.11 Overlapping index of grain flow lines

1.3 Optimal design of clinching process considering joining strength

Figure 1.12-1.14 shows process optimal design of the clinching process considering the joint strength. Figure 1.12 summarizes the process setup and the design variables. As shown in Figure 1.13, the joint strength was calculated by adding another stage with two dies. The upper die of the second stage will exert a tensile force on the clinched joint to evaluate the joint strength. The effective strain and effective stress distributions as a result of the analysis of the forming and separation processes are plotted in Figure 1.13.

The forming load of the second stage, which physically means the joint strength, is defined as the objective function. The goal is to maximize the objective function, thereby getting a stronger clinched joint. Through this optimization process, the initial joint strength of 1.61 kN was increased up to 2.20 kN as can be seen in Figure 1.14.

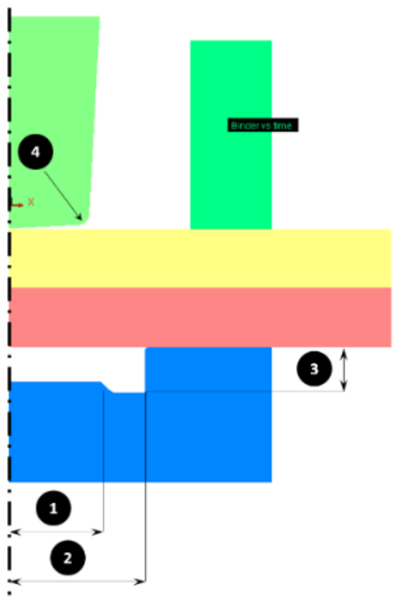

No	Parameter	Initial	Minimum	Maximum
1	Die base width	4.00	3.80	4.20
2	Die radius	5.84	5.54	6.14
3	Die depth	7.94	7.64	8.24
4	Punch radius	0.50	0.20	0.80

(All dimensions are in mm)

Fig. 1.12 Process setup and design variables

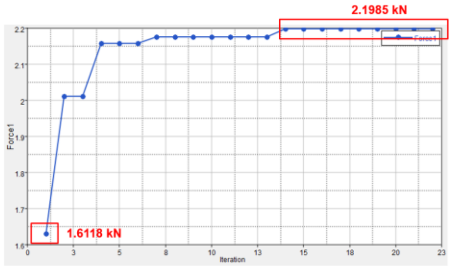

Fig. 1.13 Optimization of joining strength

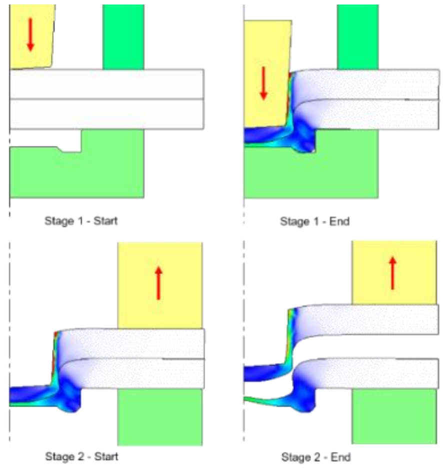

(a) Effective strain predictions

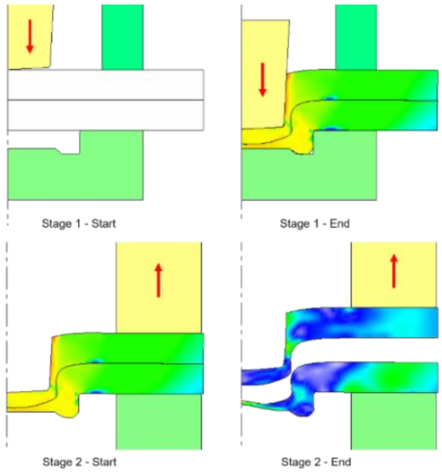

(b) Effective stress predictions

Figure 1.14 FE Predictions of the process

2. 3D shearing, piercing and trimming process analysis

2.1 Summary

3D analysis of shearing, piercing, and trimming processes is not easy because of complicated fracture theory and mesh generation problem. However, the analysis of shearing, piercing, and trimming in the actual metal forming process is very important. Especially, when the sheared blank shape is greatly affected by shearing condition of plate forging process, the analysis like shearing process is very important. Recently, AFDEX developed the analysis technique for shearing, piercing, blanking and trimming process, which is theoretically based on the ductile fracture theory and element degradation technique. Also, extreme mesh density control for remeshing is applied to minimize the deterioration in surface smoothness after removing damaged element.

Here, three typical applications are introduced. (KSTP Fall Conference, Jeju Island, 2018.10.11).

2.2 Shearing process

Figure 2.1 compares FE predictions with experiments of the material cutting process in a multi-stage automatic cold forging process. A characteristic of this analysis is that the cut surfaces have been appropriately refined so that the cut material can be used for the analysis of subsequent process. In other words, as shown in the figure, the overall analysis results are in good agreement with the experimental results, but the surface treatment has been performed for the success of the analysis of subsequent process (KSTP Fall Conference, Jeju Island, 2018.10.11).

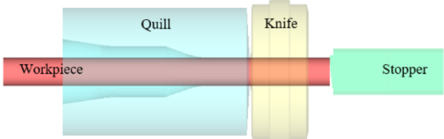

(a) Process schematic

(b) FE Prediction

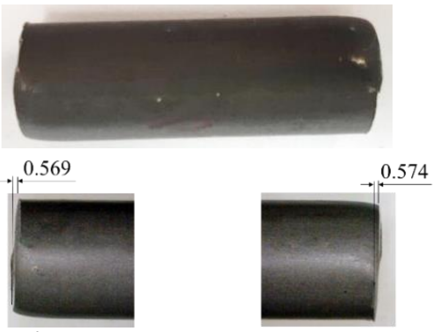

(c) Experiment

Figure 2.1 Analysis of cold cutting process of bar and comparison with experiment results

2.3 Analysis of piercing/trimming process

Figure 2.2 shows the predictions of the piercing process, and Figure 2.3 shows those of the trimming process. Both examples used dense elements at the cutting area, and the element quality was good enough at the cut surface.

Figure 2.2 shows the piercing process in the thick plate, where the cross section is visualized.

Figure 2.3 shows the trimming process in which material separation occurs in most of the regions in a short time, but trimmed shape near the corner of the material showed very sharp edge. (KSTP Fall Conference, Jeju Island, 2018.10.12).

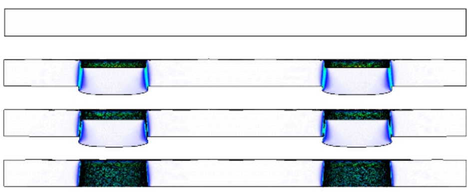

(a) Global view

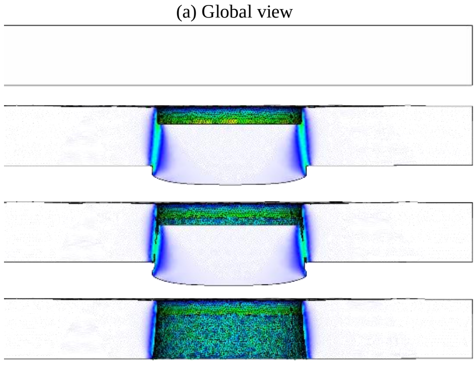

(b) Local view

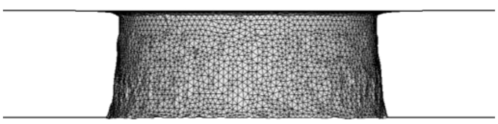

(c) Detailed view

Figure 2.2 Analysis result of piercing process

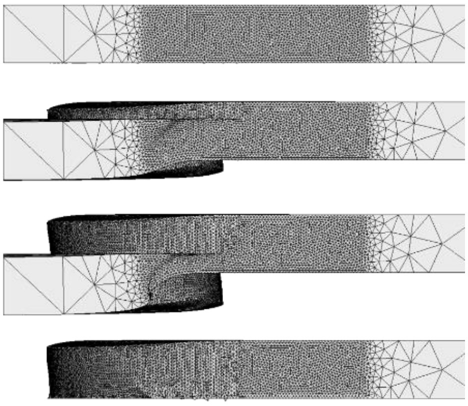

(a) Side view

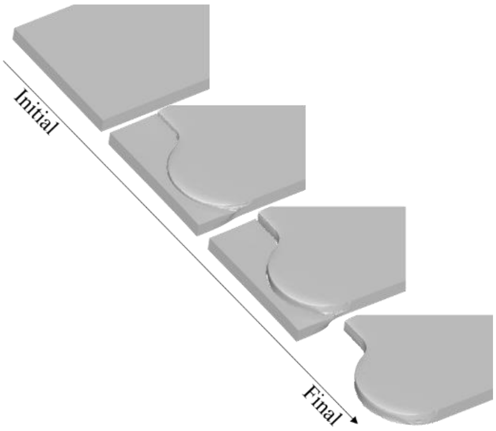

(b) Bird's eye view

Figure 2.3 Analysis result of trimming process

3. Remesh in 3D multi-body process analysis

The rigid and elasto-plastic finite element analysis of 3D multibody processes have already been introduced in the second quarter of the 2018 newsletter. This module is not tied to the automatic remesh function, which is constrained in utilization and is not yet open to the user for that reason.

Recently, the module for the analysis of 3D multi-body process has been connected with remeshing so that the automatic analysis of the whole process is possible without user intervention. Also, the usability was improved by generalizing the input data structure. Figure 3.1 and Figure 3.2 show a typical application example.

Figure 3.1 is an upsetting process for two materials with different sizes and flow stresses to introduce the concept of multibody process. Although this process is a simple process in terms of shape, it is a problem that is numerically difficult due to the symmetry plane and sharp corner. With 12 times of remeshing during simulation, it was confirmed that the numerical treatment works well especially on the contact surface and the symmetric surface.

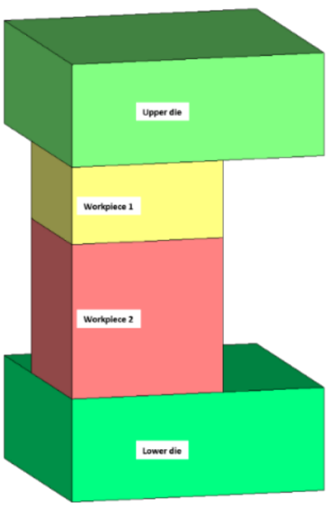

(a) Initial condition

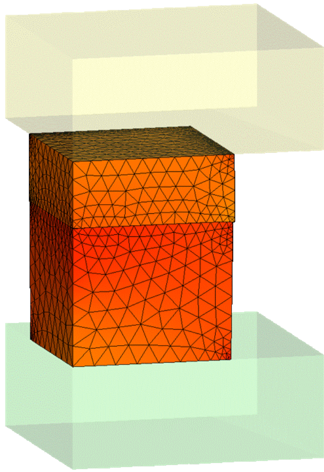

(b) Simulation result

Fig. 3.1 Upsetting of two rectangular tetrahedral objects

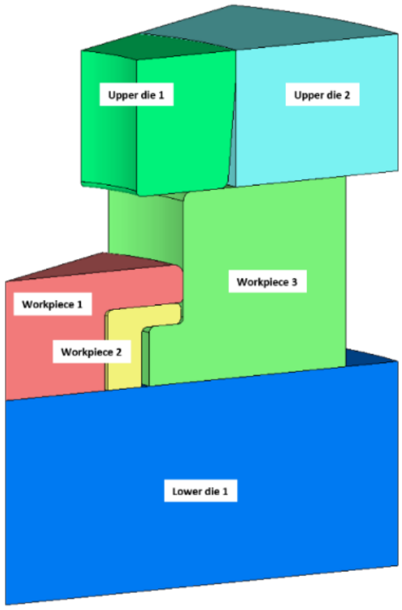

(a) Initial condition

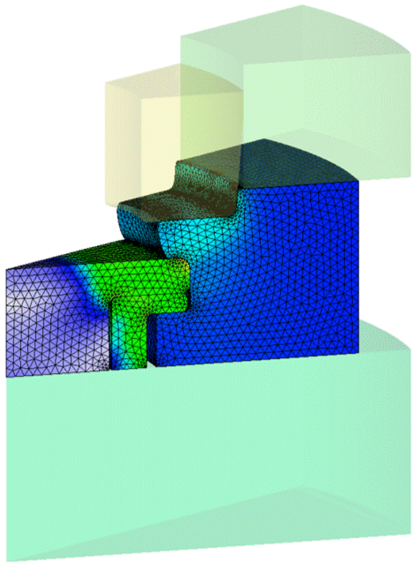

(b) Simulation result

Fig. 3.2 Assembly process of virtual three objects

Figure 3.2 is a virtual process of assembling three objects. The axisymmetric process is analyzed by using the 3D multibody analysis function. A total of 7 remeshings were performed due to the characteristics of the process. This example can be simulated by a 2D analysis function, and the 2D analysis result is quantitatively similar to the 3D analysis result.

The 3D multibody analysis function is essential for the prediction of the clamping force during the assembly process with the already announced 2D multibody analysis function. In the case of the special process, it can be simulated under the same treatment conditions for die and material.

This function will be available to users of the AFDEX / Pro version starting with V19R01 (to be released on March 1st, 2019).

4. Notice

4.1 MFCAE 2018

MFCAE 2018 was held at Pearl MBC Convention on 16,17 August 2018. At this event, undergraduate sessions, graduate student sessions, developer sessions, and professional training sessions were held. Chief developer Dr. ManSoo Joun gave a special lecture on the simulation technology of metal forming processes.

Fig. 4.1 MFCAE 2018

4.2 Altair Technology Conference 2018 Korea

Dr. Suk-hwan Chung attended the ATC 2018 held on September 14, 2018 at Altair Korea in Conrad Hotel, Yeouido, Seoul. This event introduces various customer cases using digital twin, which is emerging as a big issue in recent manufacturing industry with the theme of "product development and digital twin". (Link: http://blog.altair.co.kr/54694)

He has presented the subject of 'Optimal design of grain flow lines in forging process for bearing using AFDEX and HyperStudy ' in Manufacturing Session.

Fig. 4.2 ATC 2018 Korea

4.3 Global Altair Technology Conference 2018

The 2018 Global Altair Technology Conference will be held in Paris, France from October 16 to 18. The ATC is a comprehensive CAE conference led by Altair and involving key Altair APA partners and users across the globe. MFRC would be participating in the event as an exhibitor and our team looks forward to meeting with our global users as well as people from the simulation community. MFRC will announce new features such as multi-body simulation and heat treatment module through this event.

4.4 Training program at Altair headquarters

A 2-day training on the basics of AFDEX and forging simulation technology will be conducted at Altair Headquarters starting from 24th October. The course will have a mix of theory (fundamentals of forging simulation, AFDEX basics, etc.) as well as practice sessions, where the attendees would get a chance to simulate the processes in AFDEX. Three researchers from MFRC including Dr. ManSoo Joun, the CEO of MFRC will conduct the training program. If you are interested in participating, kindly use the link below for registration. (Link)

4.5 Altair education event in Canada

MFRC would also be conducting a one-day training program on 26th of October at Altair's Toronto office. In addition to the introduction of simulation technology and AFDEX, this event will have a practice session too where attendees get to lay their hands on AFDEX and try out some new and exciting features. This is a great opportunity for our team to interact in person with our growing user base in Canada. Visit the link below to know more about the event and if you are interested, please register there as well. (Link)

4.6 AFDEX training programs in Mexico

A 2-day training program will be organized in Mexico City on 29 and 30th of October. The first day of the training will be held at Hotel Camino Real AeroPuerto and the second day which will consist of AFDEX practice, will be held at the AFDEX Center in UPVM, Mexico City.

This event will be followed a 1-day training program at the industrial region of Ciudad Juarez on 31st of October. Interested participants can visit our website to know further details. The link below can be used for registration purpose. All the events in Mexico are held and organized jointly with UPVM and Altair Mexico. (Link)

4.7 EuroForge

EuroForge conFAIR will be held for the first time in Berlin, Germany for three days starting from 13th of November. It is composed of exhibitions of industrial companies in the forging industry, and presentation on the latest forging technology, light weighting, forging industry 4.0, and global market trends.

MFRC will participate as a platinum sponsor, and Dr. ManSoo Joun and three other researchers will present a paper on process optimization.